Published in final edited form as:
Dev Biol. 2012 February 1; 362(1): 57–64. doi:10.1016/j.ydbio.2011.11.010.

Ongoing Notch signaling maintains phenotypic fidelity in the adult exocrine pancreas

Daniel Kopinke[1], **Marisa Brailsford**[1], **Fong Cheng Pan**[2], **Mark A. Magnuson**[2,3], **Christopher V.E. Wright**[2], and **L. Charles Murtaugh**[1,*]

[1]Department of Human Genetics, University of Utah, 15 North 2030 East, Salt Lake City, UT 84112

[2]Department of Cell and Developmental Biology, Vanderbilt University Medical Center, Nashville, TN 37232

[3]Department of Molecular Physiology and Biophysics, Vanderbilt University Medical Center, Nashville, TN 37232

Abstract

The Notch signaling pathway regulates embryonic development of the pancreas, inhibiting progenitor differentiation into exocrine acinar and endocrine islet cells. The adult pancreas appears to lack progenitor cells, and its mature cell types are maintained by the proliferation of pre-existing differentiated cells. Nonetheless, Notch remains active in adult duct and terminal duct/centroacinar cells (CACs), in which its function is unknown. We previously developed mice in which cells expressing the Notch target gene *Hes1* can be labeled and manipulated, by expression of Cre recombinase, and demonstrated that *Hes1*$^+$ CACs do not behave as acinar or islet progenitors in the uninjured pancreas, or as islet progenitors after pancreatic duct ligation. In the current study, we assessed the function of Notch signaling in the adult pancreas by deleting the transcription factor partner of Notch, *Rbpj*, specifically in *Hes1*$^+$ cells. We find that loss of *Rbpj* depletes the pancreas of *Hes1*-expressing CACs, abrogating their ongoing contribution to growth and homeostasis of more proximal duct structures. Upon *Rbpj* deletion, CACs undergo a rapid transformation into acinar cells, suggesting that constitutive Notch activity suppresses the acinar differentiation potential of CACs. Together, our data provide direct evidence of an endogenous genetic program to control interconversion of cell fates in the adult pancreas.

Keywords

pancreas; Notch; *Rbpj*; transdifferentiation; acinar; centroacinar

INTRODUCTION

The adult pancreas experiences relatively little cell turnover during normal homeostasis, and most evidence to date indicates that its cell types are maintained by faithful replication of pre-existing cells. In endocrine islets, replication is the main mode of generating new

*corresponding author, tel. 801-581-5958, murtaugh@genetics.utah.edu.

insulin-producing β-cells (Brennand et al., 2007; Dor et al., 2004; Georgia and Bhushan, 2004; Teta et al., 2007). Replication also appears to be the mechanism by which acinar cells, belonging to the exocrine pancreas, are maintained during homeostasis and regeneration (Desai et al., 2007; Strobel et al., 2007). Although it remains controversial whether adult stem or progenitor cells contribute to maintenance and repair of the pancreas, embryonic pancreatic organogenesis relies on multipotent and lineage-restricted progenitor cells, the differentiation of which is controlled by intrinsic and extrinsic factors (reviewed in Pan and Wright, 2011). Notch signaling is a major regulator of progenitor cell differentiation, in the embryonic pancreas as well as numerous other developing and adult tissues (Chiba, 2006). Although Notch appears to be active in the adult pancreas, its potential contribution to tissue homeostasis is unknown and is the focus of this study.

The Notch pathway is activated by juxtacrine interactions between Delta/Serrate family ligands and Notch family receptors, which trigger the protease-induced release and nuclear translocation of the Notch intracellular domain (NIC). Nuclear NIC binds the transcription factor Su(H)/CSL/Rbpjκ (henceforth referred to as Rbpj), and co-activates target genes including the Hes/Hey family of transcriptional repressors (Kageyama et al., 2007; Kopan and Ilagan, 2009). A central output of Notch signaling, across tissues and phyla, is control of cell fate (Chiba, 2006), and Notch activation in the embryonic pancreas inhibits acinar and islet cell differentiation while promoting development of duct cells (Esni et al., 2004; Hald et al., 2003; Kopinke et al., 2011; Murtaugh et al., 2003; Yee et al., 2005). In the mature pancreas, gain-offunction studies suggest that Notch signaling promotes acinar cell transdifferentiation to duct or progenitor-like cells (De La O et al., 2008; Miyamoto et al., 2003; Mukhi and Brown, 2011). Whether endogenous Notch plays such a role remains unclear, as the only phenotype observed after pan-pancreatic deletion of the *Notch1* receptor is impaired regeneration of adult acinar cells (Siveke et al., 2008). Nonetheless, Notch signaling appears to be active in the adult pancreas, as evidenced by expression of its target gene *Hes1* in centroacinar cells (CACs) and ducts (Kopinke et al., 2011; Miyamoto et al., 2003; Parsons et al., 2009; Stanger et al., 2005). CACs constitute the terminal element of the ductal tree and are characterized by their central position within individual acinar rosettes (Ekholm et al., 1962). These cells have been proposed to represent an adult progenitor-like cell in the pancreas and to produce new β-cells following injury (Hayashi et al., 2003; Nagasao et al., 2003) and in vitro (Rovira et al., 2010). Whether CACs actually behave as adult progenitor cells in vivo has remained controversial, as tools for lineage tracing these cells have been lacking until now.

We recently generated a tamoxifen-inducible Cre line under the control of the *Hes1* promoter (*Hes1*^{CreERT2}, abbreviated *Hes1*^{C2}), which faithfully marks *Hes1*$^{+}$ CACs (Kopinke et al., 2011). Lineage tracing experiments in adult mice indicate that adult *Hes1*$^{+}$ CACs do not normally contribute to new β-cells or acini. In utero, however, *Hes1*$^{+}$ cells represent bipotent exocrine progenitors in which ectopic Notch promotes duct specification at the expense of acinar fate (Kopinke et al., 2011). Thus, sustained Notch signaling in *Hes1*$^{+}$ CACs might enforce their ductal fate and restrain their full differentiation potential. In the current study, we challenge the system by disrupting Notch signaling specifically in *Hes1*-expressing cells, and demonstrate that Notch controls interconversion of cell fates in the adult pancreas.

MATERIAL AND METHODS

Animal experiments

Hes1^{C2} (Kopinke et al., 2011), *R26R*^{EYFP} (Srinivas et al., 2001) and *Rbpj* ^{lox} (Han et al., 2002) mice have been described previously. *Ptf1a*$^{Cre-ERTM}$ mice were generated by recombinase-mediated cassette exchange (Burlison et al., 2008), inserting the Cre-ERTM

coding region (Danielian et al., 1998) into the first exon of *Ptf1a* (full details of this allele will be published elsewhere). *Rbpj* ^{lox} mice, kindly provided by Tasuku Honjo (Kyoto University, Kyoto, Japan) and Sean Morrison (University of Michigan, Ann Arbor, MI), were crossed to *Hprt*-Cre deletor mice (Tang et al., 2002) to generate a null (*Rbpj*$^{\Delta}$) allele. PCR genotyping for the floxed allele of *Rbpj* was performed as described (Han et al., 2002); for the null allele, the following oligos were used: forward 5'-TAACTATCTTGGAAGGCTAAAAT-3' and reverse 5'-GCTTGAGGCTTGATGTTCTGTATTGC-3' (598 bp product).

Tamoxifen (Sigma T-5648) was dissolved in corn oil, and administered by oral gavage at doses of 5 mg (*Ptf1a*$^{Cre\text{-}ERTM}$) or 10 mg (*Hes1*^{C2}) per mouse between 6–8 weeks of age. BrdU (Sigma) was dissolved in drinking water (1 mg/ml) and provided to mice ad libitum, beginning 3 days prior to tamoxifen administration and continuing for 7 days thereafter. All animal procedures were approved by the Institutional Animal Care and Use Committee of the University of Utah.

Staining and analysis

Immunostaining and analysis were performed as previously described (Kopinke et al., 2011; Kopinke and Murtaugh, 2010). The following primary antibodies were used: sheep anti-amylase 1:2500 (BioGenesis), rat anti-BrdU 1:2000 (Abcam), rabbit anti-cytokeratin-19 1:1500 (gift from Ben Stanger, University of Pennsylvania, Philadelphia, PA), rabbit monoclonal anticytokeratin-19 1:500 (Epitomics), rat anti-cytokeratin-19 1:50 (Developmental Studies Hybridoma Bank), rabbit anti-cleaved Caspase3 1:1000 (Cell Signaling), rat anti-E-cadherin 1:2000 (Zymed), rabbit anti-GFP 1:4000 (Abcam), goat anti-GFP 1:2500 (Rockland), guinea pig anti-glucagon 1:2500 (Linco), rabbit anti-glucagon 1:2500 (Zymed), guinea pig anti-Insulin 1:2000 (Dako), rabbit anti-Ki67 1:150 (Vector labs) and rabbit anti-Ptf1a 1:800 (gift from Helena Edlund, Umea University, Umea, Sweden). All secondary antibodies (raised in donkey) were obtained from Jackson Immunoresearch. For Ki67 and BrdU immunofluorescence, a 15 min DNase I digestion (700 U/μl, in 40 mM Tris-HCl pH 7.4, 10 mM NaCl, 6 mM $MgCl_2$, 10 mM $CaCl_2$) was necessary (Ye et al., 2007). Periodic Acid Schiff (PAS) staining was carried out according to the manufacturer's instructions (Sigma). For quantifications, co-immunofluorescence was determined using the Analyze Particles function of ImageJ (NIH) and confirmed by eye in Adobe Photoshop. Calculations and graphs were generated with Microsoft Excel and R (www.r-project.org). *P*-values were determined by Tukey's HSD test in R, and data are represented as mean +/− SEM. The numbers of mice used for each experiment are indicated in each graph. Acinar dissociation was performed as previously described (Kopinke and Murtaugh, 2010). The total number of cells counted for each graph is listed in Table S1.

RESULTS

Hes1-specific deletion of *Rbpj* in adult intestine and pancreas

Rbpj encodes the transcription factor through which Notch activates target genes (Kopan and Ilagan, 2009). To determine a potential role for Notch signaling in *Hes1*$^{+}$ cells of the adult pancreas, we used our inducible *Hes1*^{CreERT2} line (*Hes1*^{C2}) to delete a floxed *Rbpj* allele (Han et al., 2002; Kopinke et al., 2011). Our breeding scheme (Fig. 1A) yielded both *Hes1*$^{C2/+}$*; Rbpj*$^{lox/+}$ mice, which are heterozygous for the floxed allele (henceforth referred to as *Rbpj*$^{Hes1\text{-}lox}$), and *Hes1*$^{C2/+}$*; Rbpj* $^{lox/\Delta}$ animals, which carry a null (Δ) and a floxed allele of *Rbpj* (*Rbpj*$^{Hes1\text{-}cKO}$). All genotypes also included an *R26R*^{EYFP} reporter (Srinivas et al., 2001), to follow the fate of recombined cells (see below). *Rbpj*$^{Hes1\text{-}cKO}$ mice reached adulthood at a Mendelian ratio, and were indistinguishable from wild-type or *Rbpj*$^{Hes1\text{-}lox}$ animals before tamoxifen (TM) administration. It should be noted, however, that

Rbpj$^{Hes1\text{-}cKO}$ animals are compound heterozygotes for two major Notch components, *Hes1* and *Rbpj*. As an additional control, therefore, we generated mice that were heterozygous for the null rather than the floxed allele of *Rbpj* (*Hes1*$^{C2/+}$; *R26R*$^{EYFP/+}$; *Rbpj*$^{\Delta/+}$; referred to as *Rbpj*$^{Hes1\text{-}het}$). Comparisons between these mice and *Rbpj*$^{Hes1\text{-}cKO}$ allowed us to distinguish potential phenotypes caused by compound *Hes1/Rbpj* heterozygosity from those attributable to complete loss of *Rbpj*.

In all experiments, unless otherwise indicated, 10 mg TM was administered to 6–8 week old adult mice, which were chased for 7 days (short term) or 2 months (long term) (Fig. 1B). To monitor proliferation of labeled cells, mice used for 7 day chase experiments were also continuously supplied with the thymidine analogue BrdU in the drinking water, from 3 days prior to TM treatment through sacrifice. This approach has previously been shown to capture all cells entering S-phase during the chase period (Teta et al., 2007).

Inhibiting Notch in the small intestine causes overproduction of goblet cells (Riccio et al., 2008; van Es et al., 2005), and we assayed this phenotype as an indicator of successful *Rbpj* deletion. *Hes1*^{C2} is active in intestinal stem cells (Kopinke et al., 2011), and deletion of *Rbpj* with *Hes1*^{C2} caused robust transformation of the gut epithelium into PAS-positive goblet cells (Fig. 1C–D). Importantly, the pancreata of these mice exhibited no obvious morphological differences from controls (Fig. 1E–F). To confirm successful recombination in the pancreas, we performed PCR to detect the deletion (Δ) allele of *Rbpj* (Fig. 1G). As expected, the deletion-specific product can be detected in the pancreas and intestine of TM-treated *Rbpj*$^{Hes1\text{-}lox}$ mice, indicating recombination of the floxed allele.

Deletion of *Rbpj* in *Hes1*-expressing duct cells blocks their expansion

We previously showed that *Hes1*^{C2} marks not only CACs but also a preferentially-expanding subset of cells within adult ducts, consistent with a recent study suggesting that Jagged1-Notch signaling is mitogenic for ducts (Golson et al., 2009; Kopinke et al., 2011). We therefore analyzed *Rbpj* knockouts for any defects of the ductal tree, using the *R26R*^{EYFP} reporter allele to monitor the fate of cells deleting *Rbpj*. This approach should allow us to quantitatively compare *Rbpj*$_{Hes1\text{-}lox}$ to *Rbpj*$^{Hes1\text{-}cKO}$ cells by virtue of EYFP expression.

As previously (Kopinke et al., 2011), we could detect an increase in the fraction of labeled CK19^{+} duct cells between 7 days and 2 months in *Rbpj*$^{Hes1\text{-}lox}$ mice. By comparison, the labeling index of *Rbpj*$^{Hes1\text{-}cKO}$ ducts remained the same regardless of the chase period (Fig. 2A–E; see also Table S1 for details on this and other quantitative analyses), suggesting that the expansion of *Hes1* lineage-derived ducts requires Notch activity. The ductal tree can be divided into proximal (intra- and interlobular) and distal ducts (intercalated ducts, terminal ducts and CACs) (Kopinke and Murtaugh, 2010). To determine if loss of *Rbpj* results in different outcomes at different positions within the ductal network, we analyzed *Rbpj*$^{Hes1\text{-}lox}$ and *Rbpj*$^{Hes1\text{-}cKO}$ pancreata for the contribution of EYFP^{+} cells specifically to proximal and distal ducts at 7 days post-TM. Since terminal ducts and CACs are phenotypically similar and difficult to distinguish under the microscope (Ekholm et al., 1962), we analyzed them together and henceforth refer to them collectively as CACs. We found that although the EYFP^{+} fraction of intra- and interlobular ducts did not change within 7 days of *Rbpj* deletion (Fig. 2F), *Rbpj*-deleted intercalated ducts and CACs experienced an approximately 2-fold reduction in their EYFP labeling index (Fig. 2G). In addition, the fraction of EYFP-labeled cells that had progressed through the cell cycle, as indicated by BrdU incorporation, did not change among proximal ducts but decreased ~2-fold in distal ducts (Fig. 2F–I).

In wild-type pancreata, both the EYFP and BrdU labeling indices of distal duct cells are approximately double those of proximal cells (Fig. 2F–G). The fact that proliferation of

distal cells declined to a more proximal-like level, following *Rbpj* deletion, could reflect a mitogenic role for Notch in this population, but a change in proliferation alone seemed insufficient to explain the observed rapid decrease in EYFP labeling of distal duct cells. Staining for cleaved Caspase-3 revealed minimal apoptosis in either genotype, after a 2 or 7 day post-TM chase, with no increase upon *Rbpj* deletion (Fig. S1 and data not shown), suggesting that apoptosis was not responsible for the disappearance of labeled cells from the distal ducts. To determine if loss of *Rbpj* might cause necrosis or other injury of duct cells, we stained for the exocrine lumenal marker Muc1, which is expressed preferentially in distal ducts and acini (Kopinke and Murtaugh, 2010). Consistent with the normal histological appearance of $Rbpj^{Hes1\text{-}cKO}$ pancreata (Fig. 1E–F), we found no gross or subtle morphological abnormalities in the $Muc1^{+}$ ductal network following *Rbpj* deletion (Fig. S2). We therefore considered the possibility that a subset of *Rbpj*-depleted distal duct cells had adopted a non-ductal fate.

Dramatic increase of *Hes1*-labeled acinar cells after loss of *Rbpj*

Notch signaling inhibits embryonic islet cell development (Apelqvist et al., 1999; Jensen et al., 2000), suggesting that *Rbpj*-deleted CACs might adopt an endocrine fate. Nonetheless, we did not detect a single insulin^{+} β-cell labeled by EYFP after a 7-day or 2-month chase in $Rbpj^{Hes1\text{-}cKO}$ mice, nor was there any increase in the small fraction of glucagon^{+} α-cells normally labeled by $Hes1^{C2}$ (Kopinke et al., 2011) (Fig. S3). We conclude that inhibiting Notch activity does not permit CAC-to-islet differentiation. By contrast, casual inspection revealed a considerable increase in EYFP labeling of $Rbpj^{Hes1\text{-}cKO}$ acinar cells compared to $Rbpj^{Hes1\text{-}lox}$ (Fig. 3A–D). This effect was quite rapid: within 7 days of tamoxifen administration, $Rbpj^{Hes1\text{-}cKO}$ pancreata exhibited an approximately 3.5-fold increase in labeled acinar cells, which did not increase further after 2 months (Fig. 3E). This increase was not due to compound haploinsufficiency for *Rbpj* and *Hes1*, as the acinar labeling index of $Rbpj^{Hes1\text{-}het}$ mice was indistinguishable from $Rbpj^{Hes1\text{-}lox}$. The increase in EYFP^{+} acinar cells was not accompanied by a detectable change in total pancreas mass despite what should correspond to a 10% increase in total acinar numbers (Fig. S4), although such a small change might be difficult to detect in the face of even modest experimental noise.

Notch signaling has previously been suggested to inhibit acinar cell proliferation (Siveke et al., 2008). To determine whether the increased acinar labeling in $Rbpj^{Hes1\text{-}cKO}$ could be attributed entirely to division of rare $Hes1^{C2}$-labeled acinar cells (Kopinke et al., 2011), we analyzed BrdU incorporation rates in $Rbpj^{Hes1\text{-}lox}$ and $Rbpj^{Hes1\text{-}cKO}$ mice (see above). After a 7 day chase, ~2% of EYFP^{+} acinar cells were positive for BrdU in $Rbpj^{Hes1\text{-}lox}$ mice, compared to ~4% in $Rbpj^{Hes1\text{-}cKO}$ mice (Fig. 3G–I). Because the initial fraction of BrdU^{+} acinar cells even after continuous administration of BrdU for 10 days was very low, and increased only to 4% in $Rbpj^{Hes1\text{-}cKO}$ mice, accelerated proliferation of $Hes1^{+}$ acinar cells cannot explain fully the dramatic increase in EYFP^{+} acinar cells following *Rbpj* deletion.

To analyze acinar cells more directly, we deleted *Rbpj* using a TM-inducible Cre line under control of the acinar-specific transcription factor *Ptf1a* ($Ptf1a^{Cre\text{-}ERTM}$) (Fig. 4A). Immunostaining confirmed that all acinar cells expressed Ptf1a, including the subpopulation labeled by $Hes1^{C2}$ (Fig 4B). Similar to our $Hes1^{C2}$ breeding scheme (Fig. 1A), we generated mice containing floxed and wild-type *Rbpj* alleles ($Rbpj^{Ptf1a\text{-}lox}$), or floxed and null alleles ($Rbpj^{Ptf1a\text{-}cKO}$), all on a $R26R^{EYFP/+}$ background (Fig. 4A). We found no difference between $Rbpj^{Ptf1a\text{-}lox}$ and $Rbpj^{Ptf1a\text{-}cKO}$ in the EYFP labeling of acinar cells at 7 days post-TM (Fig. 4C–E). Using the same BrdU labeling scheme as above, we also detected no change in the fraction of EYFP-expressing, BrdU^{+} acinar cells between genotypes (Fig. 4F). These results argue against a role for Notch in regulating proliferation of mature acinar cells, and raise the possibility of a Notch-regulated influx to the acinar compartment from another cell type.

Loss of *Rbpj* causes rapid transformation of CAC into acinar cells

The disappearance of EYFP$^+$ intercalated ducts and CACs (Fig. 2), and our finding that Notch does not inhibit acinar proliferation (Fig. 4), prompted us to investigate whether the observed increase of EYFP$^+$ acinar cells in *Rbpj*$^{Hes1\text{-}cKO}$ mice was due to a cell fate switch of CACs (Fig. 5A). To analyze individual acinar units, and avoid missing small CACs due to sectioning artifacts, we performed enzymatic digestion to dissociate the pancreas into clusters containing only acinar cells and CACs (referred to as acinar preps; Fig. 5B) (Kopinke and Murtaugh, 2010; Kurup and Bhonde, 2002). Immediately after digestion, acinar preps were spun onto slides, fixed and processed for immunostaining. Using this method, we scored two major categories of clusters at 7 days post-TM treatment, based on the presence (class 1) or absence (class 2) of EYFP-labeled CACs. Class 1 comprised clusters in which only CACs were labeled (1a) or in which both CACs and acini were labeled (1b). Class 2 comprised clusters containing labeled acini with unlabeled CACs (2a) or labeled acini with no CACs at all (2b). If CACs were converting to acinar cells after *Rbpj* deletion, we would expect a decrease in class 1 clusters and an increase in class 2. Indeed, we found that the majority of *Rbpj*$^{Hes1\text{-}lox}$ clusters were of class 1, while class 2 predominated in *Rbpj*$^{Hes1\text{-}cKO}$ (Fig. 5G–H). Quantification revealed a 3.5-fold reduction, in *Rbpj*$^{Hes1\text{-}cKO}$ mice, of the class 1 cluster frequency, and a concomitant increase (2.5-fold) of class 2 clusters (Fig. 5I), suggesting that CACs convert to acinar cells after loss of *Rbpj*.

If CACs were indeed capable of adopting an acinar fate, we should observe transitional cells expressing both duct and acinar markers. By analyzing acinar preps from a 48 hr chase, we were able to detect EYFP$^+$ cells co-expressing the duct marker CK19 and the mature acinar marker amylase in *Rbpj*$^{Hes1\text{-}cKO}$ mice specifically (Fig. 5J–K). At later chase time points, we no longer observed EYFP-labeled cells co-expressing CK19 and amylase, nor were such cells observed in *Rbpj*$^{Hes1\text{-}lox}$ acinar preps at any time point. Thus, loss of *Rbpj* in CACs causes a rapid transition to an acinar fate.

DISCUSSION

The mammalian pancreas is a generally static organ, and numerous studies support replication as the major mode of postnatal expansion, adult homeostasis and regeneration (Brennand et al., 2007; Desai et al., 2007; Dor et al., 2004; Georgia and Bhushan, 2004; Kopinke and Murtaugh, 2010; Solar et al., 2009; Strobel et al., 2007; Teta et al., 2007). Nonetheless, adult cell fates can be overridden by the ectopic activation of developmental regulatory factors (Collombat et al., 2009; De La O et al., 2008; Zhou et al., 2008). While such gain-of-function experiments reveal the potential of adult cells to change fates, they do not address the mechanisms by which lineages normally maintain phenotypic fidelity. Here, we provide evidence that an endogenous signaling pathway acts to prevent cell type interconversion in the adult pancreas.

Notch signaling regulates cell fate decisions in numerous contexts, in some cases promoting one fate at the expense of another while in others suppressing differentiation altogether (Chiba, 2006). In the intestine, for example, Notch is not only required for absorptive cell specification but also to maintain a self-renewing stem cell compartment (Riccio et al., 2008; van Es et al., 2005). Similarly, Notch acts during early pancreas development to suppress progenitor cell differentiation, while in later organogenesis it promotes duct development at the expense of acinar (Esni et al., 2004; Hald et al., 2003; Kopinke et al., 2011; Murtaugh et al., 2003; Yee et al., 2005). We have previously shown that *Hes1* lineage-derived cells represent a preferentially expanding population within the adult duct epithelium (Kopinke et al., 2011), suggesting that Notch might act in the adult primarily as a ductal mitogen. Surprisingly, we find that although *Hes1*^{IC2} is expressed in both proximal and distal duct cells, indicating Notch activity, deletion of *Rbpj* impairs proliferation of

distal duct cells specifically (Fig. 2). These findings raise the possibility that *Rbpj*-mediated Notch signaling does not directly regulate proliferation of main duct cells, but instead drives the maintenance of a distal centroacinar cell pool that contributes to more proximal ducts during postnatal organ growth.

While this model emphasizes the cell fate determination role of Notch signaling in the adult pancreas, it leaves open the question of why CACs should retain the ability to generate acinar cells. Histological studies previously suggested that CACs could give rise to β-cells following injury, implicating this cell type as a facultative progenitor (Hayashi et al., 2003; Nagasao et al., 2003), and CACs have more recently been shown to have a unique capacity for multi-lineage differentiation in vitro (Rovira et al., 2010). Intriguingly, the cells isolated in that study were actually *Hes1*-negative (Rovira et al., 2010), consistent with the possibility that *Hes1* is normally expressed by CACs with restricted differentiation potential. It will be interesting to decipher the lineage relationship, if any, between *Hes1*-positive and -negative CACs, and to determine whether the latter population contributes to new acinar cells in vivo.

Taken together, our lineage tracing and *Rbpj* knockout results suggest that *Hes1* lineage-derived CACs behave as bipotent, exocrine-restricted progenitor cells, similar to *Hes1*-expressing cells in the late embryonic pancreas (Kopinke et al., 2011), with their acinar differentiation potential suppressed by constitutive Notch signaling. Are there circumstances in which wild-type CACs might reacquire acinar potential? One possibility is that CACs represent an "emergency reserve" for replacement of acinar cells lost to injury, and that sustained Notch signaling ensures that these cells remain available. Intriguingly, Notch activity is required for regeneration from caerulein-induced pancreatitis (Siveke et al., 2008), which might reflect the role of Notch in maintaining *Hes1*$^+$ CACs. Although lineage tracing analyses indicate that regeneration from pancreatitis is driven primarily by proliferation of surviving acinar cells (Desai et al., 2007; Strobel et al., 2007), a recent study suggests that more extreme acinar loss can be repaired by differentiation of non-acinar cells, most likely ducts (Criscimanna et al., 2011). Our findings provide a basis to address the role of *Hes1*-expressing CACs and Notch signaling in regeneration, and raise the question of whether other pathways controlling pancreatic organogenesis continue to play analogous roles in postnatal life.

HIGHLIGHTS

- Notch is required for expansion of adult pancreatic ducts
- Notch-deficient centroacinar cells do not give rise to endocrine cells
- Endogenous Notch signaling prevents centroacinar-to-acinar cell differentiation in adult pancreas

Supplementary Material

Refer to Web version on PubMed Central for supplementary material.

Acknowledgments

We thank Tasuku Honjo, Sean Morrison, Ben Stanger and Helena Edlund for generous gifts of reagents, and Nadja Makki, Jean-Paul De La O and Kristen Kwan for helpful comments on the manuscript. This work was supported by grants from the NIH (L.C.M., R01-DK075072; C.V.E.W., P01-DK42502) and Beta Cell Biology Consortium (L.C.M., U01-DK072473, subaward VUMC35146), and by graduate fellowships from the Boehringer Ingelheim Fonds and University of Utah to D.K.

REFERENCES

Apelqvist A, Li H, Sommer L, Beatus P, Anderson DJ, Honjo T, Hrabe de Angelis M, Lendahl U, Edlund H. Notch signalling controls pancreatic cell differentiation. Nature. 1999; 400:877–881. [PubMed: 10476967]

Brennand K, Huangfu D, Melton D. All beta Cells Contribute Equally to Islet Growth and Maintenance. PLoS Biol. 2007; 5:e163. [PubMed: 17535113]

Burlison JS, Long Q, Fujitani Y, Wright CV, Magnuson MA. Pdx-1 and Ptf1a concurrently determine fate specification of pancreatic multipotent progenitor cells. Dev. Biol. 2008; 316:74–86. [PubMed: 18294628]

Chiba S. Notch signaling in stem cell systems. Stem Cells. 2006; 24:2437–2447. [PubMed: 16888285]

Collombat P, Xu X, Ravassard P, Sosa-Pineda B, Dussaud S, Billestrup N, Madsen OD, Serup P, Heimberg H, Mansouri A. The ectopic expression of Pax4 in the mouse pancreas converts progenitor cells into alpha and subsequently beta cells. Cell. 2009; 138:449–462. [PubMed: 19665969]

Criscimanna A, Speicher JA, Houshmand G, Shiota C, Prasadan K, Ji B, Logsdon CD, Gittes GK, Esni F. Duct Cells Contribute to Regeneration of Endocrine and Acinar Cells Following Pancreatic Damage in Adult Mice. Gastroenterology Jul. 2011 Jul 13. [Epub ahead of print].

Danielian PS, Muccino D, Rowitch DH, Michael SK, McMahon AP. Modification of gene activity in mouse embryos in utero by a tamoxifen-inducible form of Cre recombinase. Curr. Biol. 1998; 8:1323–1326. [PubMed: 9843687]

De La O JP, Emerson LL, Goodman JL, Froebe SC, Illum BE, Curtis AB, Murtaugh LC. Notch and Kras reprogram pancreatic acinar cells to ductal intraepithelial neoplasia. Proc. Natl. Acad. Sci. U. S. A. 2008; 105:18907–18912. [PubMed: 19028876]

Desai BM, Oliver-Krasinski J, De Leon DD, Farzad C, Hong N, Leach SD, Stoffers DA. Preexisting pancreatic acinar cells contribute to acinar cell, but not islet beta cell, regeneration. J. Clin. Invest. 2007; 117:971–977. [PubMed: 17404620]

Dor Y, Brown J, Martinez OI, Melton DA. Adult pancreatic beta-cells are formed by self-duplication rather than stem-cell differentiation. Nature. 2004; 429:41–46. [PubMed: 15129273]

Ekholm R, Zelander T, Edlund Y. The ultrastructural organization of the rat exocrine pancreas. II. Centroacinar cells, intercalary and intralobular ducts. J. Ultrastruct. Res. 1962; 7:73–83.

Esni F, Ghosh B, Biankin AV, Lin JW, Albert MA, Yu X, MacDonald RJ, Civin CI, Real FX, Pack MA, Ball DW, Leach SD. Notch inhibits Ptf1 function and acinar cell differentiation in developing mouse and zebrafish pancreas. Development. 2004; 131:4213–4224. [PubMed: 15280211]

Georgia S, Bhushan A. Beta cell replication is the primary mechanism for maintaining postnatal beta cell mass. J. Clin. Invest. 2004; 114:963–968. [PubMed: 15467835]

Golson ML, Loomes KM, Oakey R, Kaestner KH. Ductal malformation and pancreatitis in mice caused by conditional Jag1 deletion. Gastroenterology. 2009; 136:1761–1771. e1761. [PubMed: 19208348]

Hald J, Hjorth JP, German MS, Madsen OD, Serup P, Jensen J. Activated Notch1 prevents differentiation of pancreatic acinar cells and attenuate endocrine development. Dev. Biol. 2003; 260:426–437. [PubMed: 12921743]

Han H, Tanigaki K, Yamamoto N, Kuroda K, Yoshimoto M, Nakahata T, Ikuta K, Honjo T. Inducible gene knockout of transcription factor recombination signal binding protein-J reveals its essential role in T versus B lineage decision. Int. Immunol. 2002; 14:637–645. [PubMed: 12039915]

Hayashi KY, Tamaki H, Handa K, Takahashi T, Kakita A, Yamashina S. Differentiation and proliferation of endocrine cells in the regenerating rat pancreas after 90% pancreatectomy. Arch. Histol. Cytol. 2003; 66:163–174. [PubMed: 12846556]

Jensen J, Pedersen EE, Galante P, Hald J, Heller RS, Ishibashi M, Kageyama R, Guillemot F, Serup P, Madsen OD. Control of endodermal endocrine development by Hes-1. Nat. Genet. 2000; 24:36–44. [PubMed: 10615124]

Kageyama R, Ohtsuka T, Kobayashi T. The Hes gene family: repressors and oscillators that orchestrate embryogenesis. Development. 2007; 134:1243–1251. [PubMed: 17329370]

Kopan R, Ilagan MX. The canonical Notch signaling pathway: unfolding the activation mechanism. Cell. 2009; 137:216–233. [PubMed: 19379690]

Kopinke D, Brailsford M, Shea JE, Leavitt R, Scaife CL, Murtaugh LC. Lineage tracing reveals the dynamic contribution of Hes1+ cells to the developing and adult pancreas. Development. 2011; 138:431–441. [PubMed: 21205788]

Kopinke D, Murtaugh LC. Exocrine-to-endocrine differentiation is detectable only prior to birth in the uninjured mouse pancreas. BMC Dev Biol. 2010; 10:38. [PubMed: 20377894]

Kurup S, Bhonde RR. Analysis and optimization of nutritional set-up for murine pancreatic acinar cells. JOP. 2002; 3:8–15. [PubMed: 11884762]

Miyamoto Y, Maitra A, Ghosh B, Zechner U, Argani P, Iacobuzio-Donahue CA, Sriuranpong V, Iso T, Meszoely IM, Wolfe MS, Hruban RH, Ball DW, Schmid RM, Leach SD. Notch mediates TGF alpha-induced changes in epithelial differentiation during pancreatic tumorigenesis. Cancer Cell. 2003; 3:565–576. [PubMed: 12842085]

Mukhi S, Brown DD. Transdifferentiation of tadpole pancreatic acinar cells to duct cells mediated by Notch and stromelysin-3. Dev. Biol. 2011; 351:311–317. [PubMed: 21194527]

Murtaugh LC, Stanger BZ, Kwan KM, Melton DA. Notch signaling controls multiple steps of pancreatic differentiation. Proc. Natl. Acad. Sci. U. S. A. 2003; 100:14920–14925. [PubMed: 14657333]

Nagasao J, Yoshioka K, Amasaki H, Mutoh K. Centroacinar and intercalated duct cells as potential precursors of pancreatic endocrine cells in rats treated with streptozotocin. Ann Anat. 2003; 185:211–216. [PubMed: 12801084]

Pan FC, Wright C. Pancreas organogenesis: From bud to plexus to gland. Dev. Dyn. 2011; 240:530–565. [PubMed: 21337462]

Parsons MJ, Pisharath H, Yusuff S, Moore JC, Siekmann AF, Lawson N, Leach SD. Notch-responsive cells initiate the secondary transition in larval zebrafish pancreas. Mech. Dev. 2009; 126:898–912. [PubMed: 19595765]

Riccio O, van Gijn ME, Bezdek AC, Pellegrinet L, van Es JH, Zimber-Strobl U, Strobl LJ, Honjo T, Clevers H, Radtke F. Loss of intestinal crypt progenitor cells owing to inactivation of both Notch1 and Notch2 is accompanied by derepression of CDK inhibitors p27Kip1 and p57Kip2. EMBO Rep. 2008; 9:377–383. [PubMed: 18274550]

Rovira M, Scott SG, Liss AS, Jensen J, Thayer SP, Leach SD. Isolation and characterization of centroacinar/terminal ductal progenitor cells in adult mouse pancreas. Proc. Natl. Acad. Sci. U. S. A. 2010; 107:75–80. [PubMed: 20018761]

Siveke JT, Lubeseder-Martellato C, Lee M, Mazur PK, Nakhai H, Radtke F, Schmid RM. Notch signaling is required for exocrine regeneration after acute pancreatitis. Gastroenterology. 2008; 134:544–555. [PubMed: 18242220]

Solar M, Cardalda C, Houbracken I, Martin M, Maestro MA, De Medts N, Xu X, Grau V, Heimberg H, Bouwens L, Ferrer J. Pancreatic exocrine duct cells give rise to insulin-producing beta cells during embryogenesis but not after birth. Dev. Cell. 2009; 17:849–860. [PubMed: 20059954]

Srinivas S, Watanabe T, Lin CS, William CM, Tanabe Y, Jessell TM, Costantini F. Cre reporter strains produced by targeted insertion of EYFP and ECFP into the ROSA26 locus. BMC Developmental Biology. 2001; 1:4. [PubMed: 11299042]

Stanger BZ, Stiles B, Lauwers GY, Bardeesy N, Mendoza M, Wang Y, Greenwood A, Cheng KH, McLaughlin M, Brown D, Depinho RA, Wu H, Melton DA, Dor Y. Pten constrains centroacinar cell expansion and malignant transformation in the pancreas. Cancer Cell. 2005; 8:185–195. [PubMed: 16169464]

Strobel O, Dor Y, Alsina J, Stirman A, Lauwers G, Trainor A, Castillo CF, Warshaw AL, Thayer SP. In vivo lineage tracing defines the role of acinar-to-ductal transdifferentiation in inflammatory ductal metaplasia. Gastroenterology. 2007; 133:1999–2009. [PubMed: 18054571]

Tang SH, Silva FJ, Tsark WM, Mann JR. A Cre/loxP-deleter transgenic line in mouse strain 129S1/SvIm. J. Genesis. 2002; 32:199–202.

Teta M, Rankin MM, Long SY, Stein GM, Kushner JA. Growth and regeneration of adult beta cells does not involve specialized progenitors. Dev. Cell. 2007; 12:817–826. [PubMed: 17488631]

van Es JH, van Gijn ME, Riccio O, van den Born M, Vooijs M, Begthel H, Cozijnsen M, Robine S, Winton DJ, Radtke F, Clevers H. Notch/gamma-secretase inhibition turns proliferative cells in intestinal crypts and adenomas into goblet cells. Nature. 2005; 435:959–963. [PubMed: 15959515]

Ye W, Mairet-Coello G, DiCicco-Bloom E. DNAse I pre-treatment markedly enhances detection of nuclear cyclin-dependent kinase inhibitor p57Kip2 and BrdU double immunostaining in embryonic rat brain. Histochem. Cell Biol. 2007; 127:195–203. [PubMed: 17024454]

Yee NS, Lorent K, Pack M. Exocrine pancreas development in zebrafish. Dev. Biol. 2005; 284:84–101. [PubMed: 15963491]

Zhou Q, Brown J, Kanarek A, Rajagopal J, Melton DA. In vivo reprogramming of adult pancreatic exocrine cells to beta-cells. Nature. 2008; 455:627–632. [PubMed: 18754011]

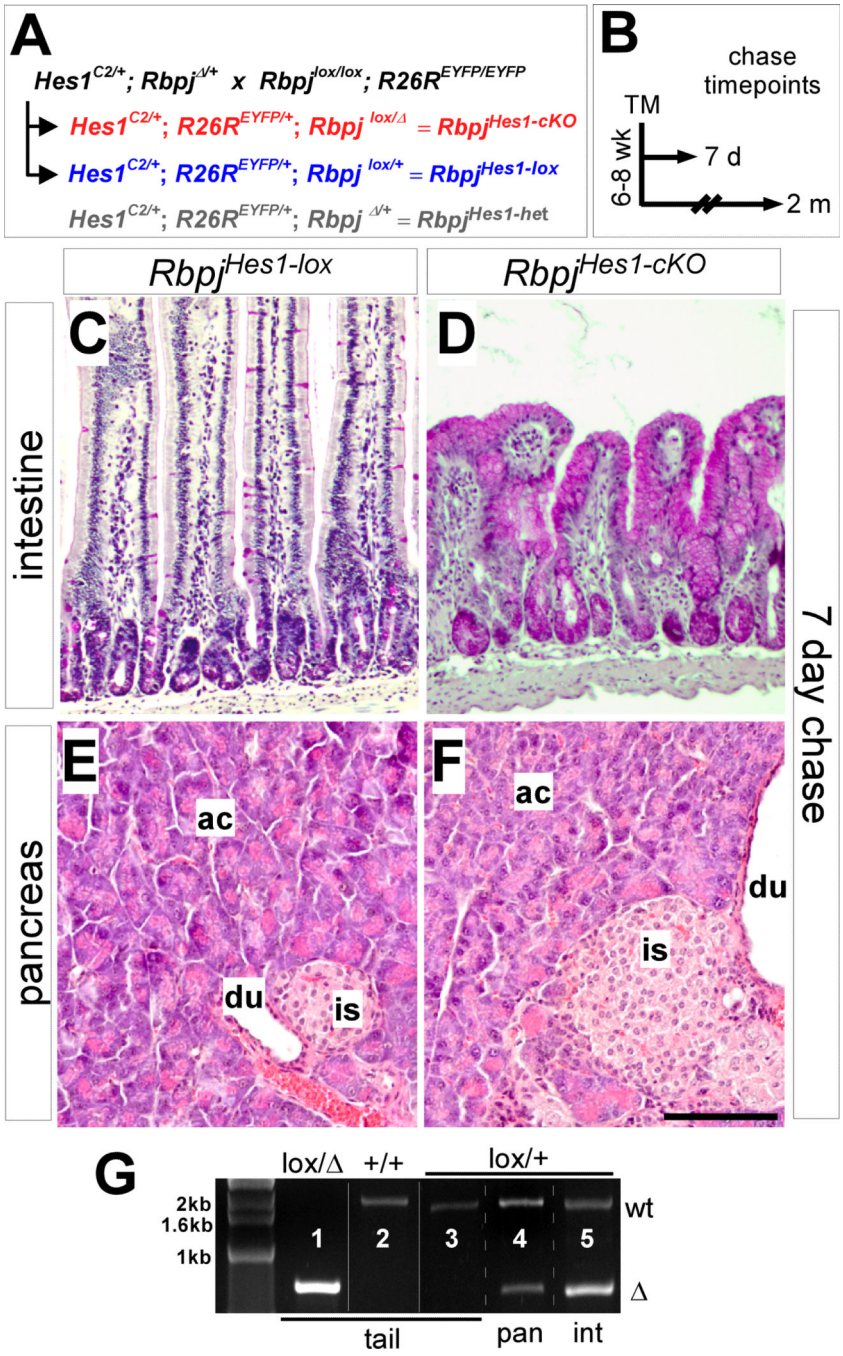

Figure 1. *Hes1*-specific deletion of *Rbpj* in the pancreas and intestine

(A) Breeding strategy for conditional knockout of *Rbpj*. Animals heterozygous for a null (Δ) and a floxed (lox) allele of *Rbpj* (*Rbpj* $^{lox/\Delta}$) are abbreviated $Rbpj^{Hes1\text{-}cKO}$, while $Rbpj^{lox/+}$ mice serve as controls ($Rbpj^{Hes1\text{-}lox}$). In some experiments, $Rbpj^{\Delta/+}$ mice were included as an additional control ($Rbpj^{Hes1\text{-}het}$). All mice also carry a $R26R^{EYFP}$ reporter allele, allowing for lineage tracing of recombined cells. **(B)** Pulse-chase strategy. Recombination was induced by TM administration in 6–8 week old adults and animals were chased for 7 days (short term) or 2 months (long term) before analyzing. **(C–F)** Comparison of PAS-stained intestine (C–D) and H&E-stained pancreata (E–F) between $Rbpj^{Hes1\text{-}lox}$ and $Rbpj^{Hes1\text{-}cKO}$ mice after a 7 day chase. Intestinal KO of *Rbpj* leads to widespread transformation of the gut

epithelium into PAS^+ goblet cells. In contrast, no morphological differences were detected between $Rbpj^{Hes1\text{-}lox}$ and $Rbpj^{Hes1\text{-}cKO}$ pancreata. **(G)** PCR to detect recombination of floxed *Rbpj*. While the deletion-specific *Rbpj* amplification product (Δ) can be detected in tail DNA from $Rbpj^{lox/\Delta}$ (lane l) but not $Rbpj^{+/+}$ or $Rbpj^{lox/+}$ (lanes 2–3) mice, the Δ band can be amplified from the pancreas or duodenum of an $Rbpj^{lox/+}$ mouse after TM treatment (lanes 4–5). Abbreviations: ac, acinar; is, islet; du, duct. Scale bar: 100 μm.

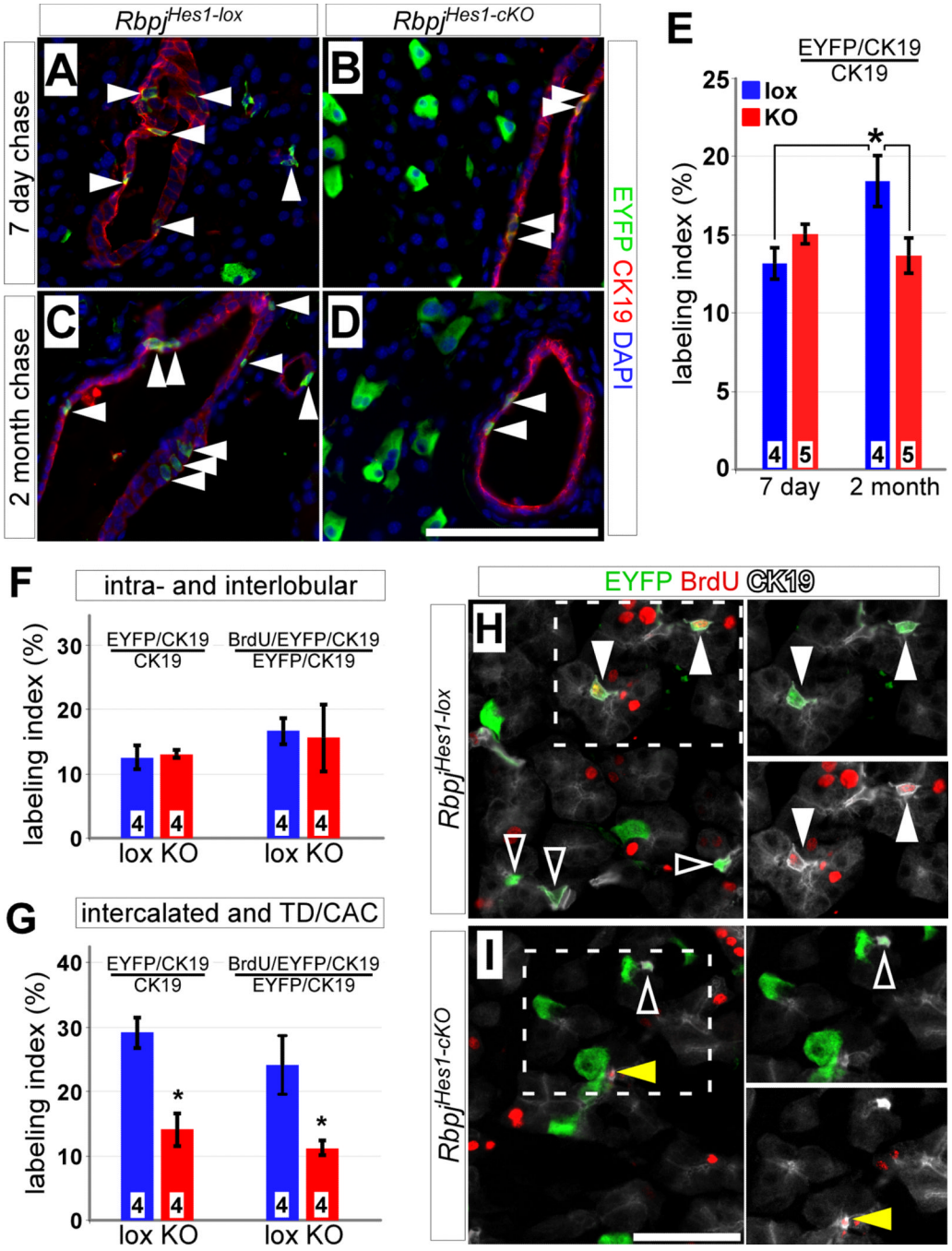

Figure 2. Deletion of *Rbpj* inhibits expansion of *Hes1*^{C2}-labeled ducts

(A–E) Adult *Rbpj*$^{Hes1\text{-}lox}$ and *Rbpj*$^{Hes1\text{-}cKO}$ mice were treated with tamoxifen and stained for EYFP (green) and the duct marker CK19 (red) after 7 days (A–B) and 2 months (C–D). While there is no difference in the fraction of EYFP-labeled duct cells (arrowheads) between 7 day chased *Rbpj*$^{Hes1\text{-}lox}$ and *Rbpj*$^{Hes1\text{-}cKO}$ animals, an increase is detected between 7 days and 2 month in *Rbpj*$^{Hes1\text{-}lox}$ mice, which is inhibited in *Rbpj*$^{Hes1\text{-}cKO}$ animals (E). * $P <$ 0.05. **(F)** Quantifications of EYFP and BrdU labeling indices of intra- and interlobular ducts indicate no differences between *Rbpj*$^{Hes1\text{-}lox}$ and *Rbpj*$^{Hes1\text{-}cKO}$ mice (P=0.75). **(G)** Quantifications of EYFP and BrdU labeling indices of intercalated ducts, terminal ducts (TD) and centroacinar cells (CACs) reveal a 2-fold decrease in EYFP labeling in

Rbpj$^{Hes1\text{-}cKO}$ mice, as well as a 2-fold reduction in the fraction of cycling (BrdU$^+$) EYFP-labeled intercalated ducts, TDs and CACs. * $P < 0.05$. **(H–I)** EYFP (green) and BrdU (red) labeling of CK19$^+$ CACs (white), 7 days post-TM and following a 10 day BrdU pulse. CACs expressing EYFP only (open arrowheads) or positive for both EYFP and BrdU (closed arrowheads) can be found in *Rbpj*$^{Hes1\text{-}lox}$ mice. In contrast, *Rbpj*$^{Hes1\text{-}cKO}$ animals have fewer EYFP$^+$ CACs, and most of the BrdU$^+$ CACs are EYFP-negative (yellow arrowhead). Numbers in bars (E–G) indicate mice analyzed per group. Scale bars: A–D and J, 100 μm; F–G, 50 μm.

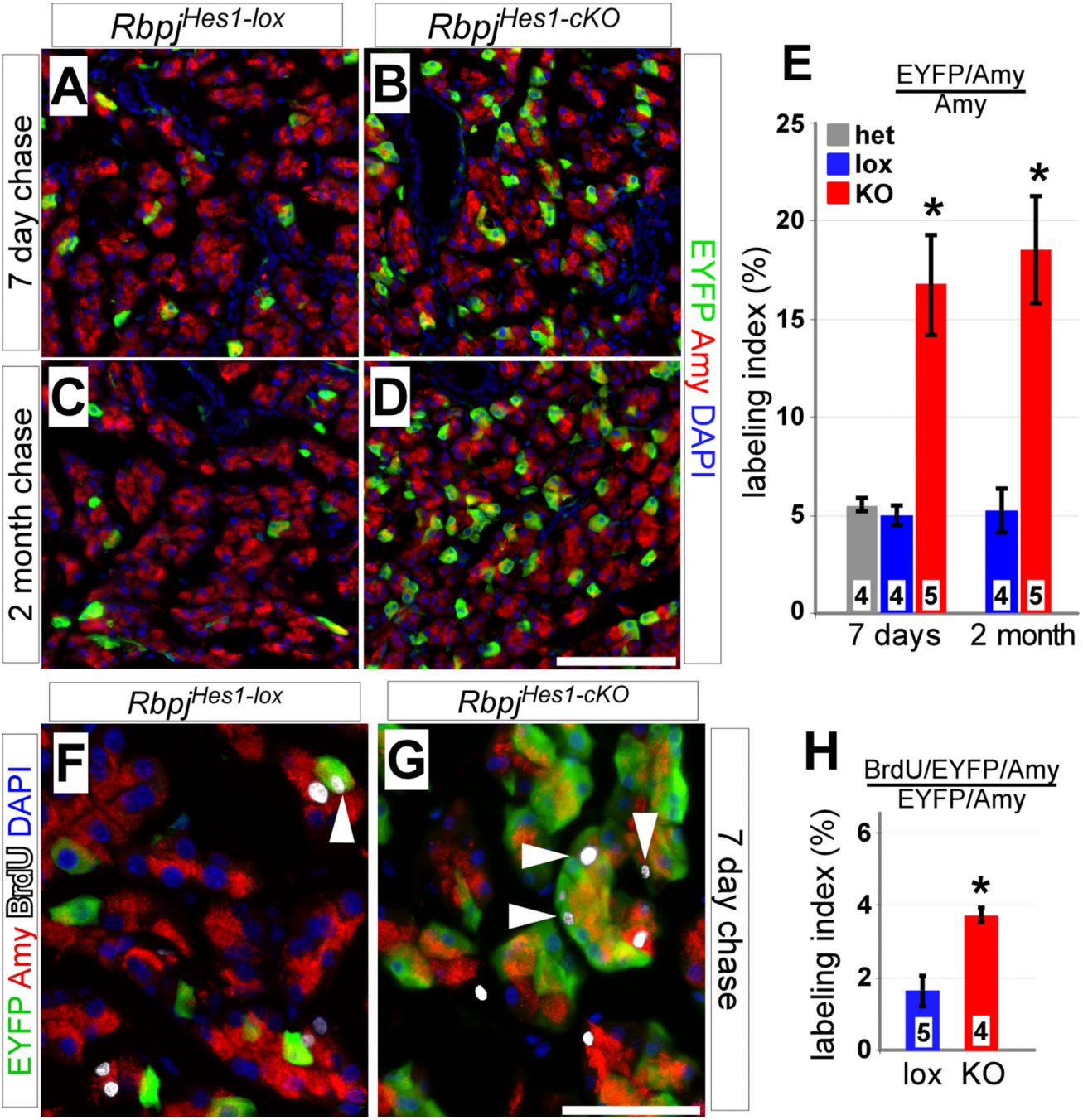

Figure 3. Loss of *Rbpj* in *Hes1*$^{+}$ cells results in dramatic increase of labeled acinar cells

(A–E) Adult *Rbpj*$^{Hes1\text{-}lox}$ and *Rbpj*$^{Hes1\text{-}cKO}$ pancreata were analyzed for co-expression of EYFP (green) with the acinar marker amylase (red), 7 days (A–B) and 2 months (C–D) post-TM. The fraction of EYFP^{+} acini in *Rbpj*$^{Hes1\text{-}lox}$ animals remains constant between 7 days and 2 months. In contrast, a drastic increase (~3.5-fold) in labeled acinar cells is seen both 7 days and 2 months after loss of *Rbpj* (E). * $P < 0.005$. **(F–H)** BrdU/EYFP labeling at 7 days post-TM. *Rbpj*$^{Hes1\text{-}cKO}$ animals display a 2-fold increase over *Rbpj*$^{Hes1\text{-}lox}$ in the fraction of EYFP^{+} acinar cells that have incorporated BrdU (white arrowheads). * $P < 0.005$. Numbers in bars (E, H) indicate mice analyzed per group. Scale bars: A–D, 100 μm; F–G, 50 μm.

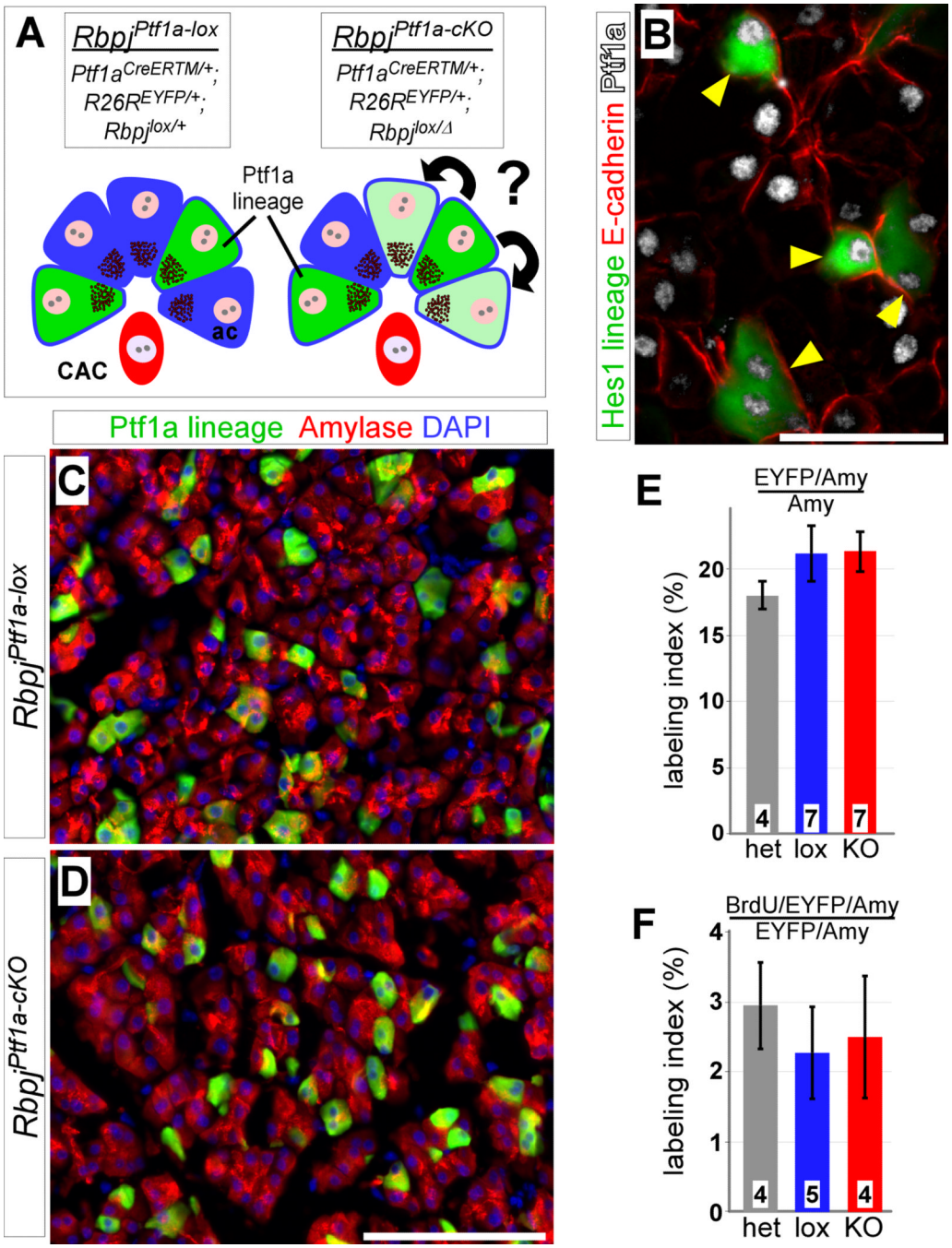

Figure 4. No increased proliferation after acinar-specific loss of *Rbpj*

(A) To determine whether Notch generally represses expansion of acinar cells, *Rbpj* was deleted using an inducible *Ptf1a*$^{Cre\text{-}ERTM}$ Cre driver, which induces mosaic recombination in acinar cells but not ducts or CACs. Blue, acinar cells; red, CAC; green, Ptf1a lineage-labeling. **(B)** Short term lineage tracing of *Hes1*$^{+}$ cells (green) demonstrates that all EYFP^{+} acinar cells (arrowheads) also express Ptf1a (white). **(C–D)** At 7 days post-TM, no difference is detected, between *Rbpj*$^{Ptf1a\text{-}lox}$ and *Rbpj*$^{Ptf1a\text{-}cKO}$, in EYFP labeling (green) of amylase^{+} acinar cells (red). **(E)** There is no change in the fraction of EYFP^{+} acinar cells after a 7 day chase (P=0.52). **(F)** Quantification of BrdU labeling analysis 7 days post-TM. The EYFP/BrdU labeling index of acinar cells remains the same between control (lox and

het) and Ptf1a1-KO animals (P=0.81). Numbers in bars (E–F) indicate mice analyzed per group. Scale bars: B, 50 μm; C–D, 100 μm.

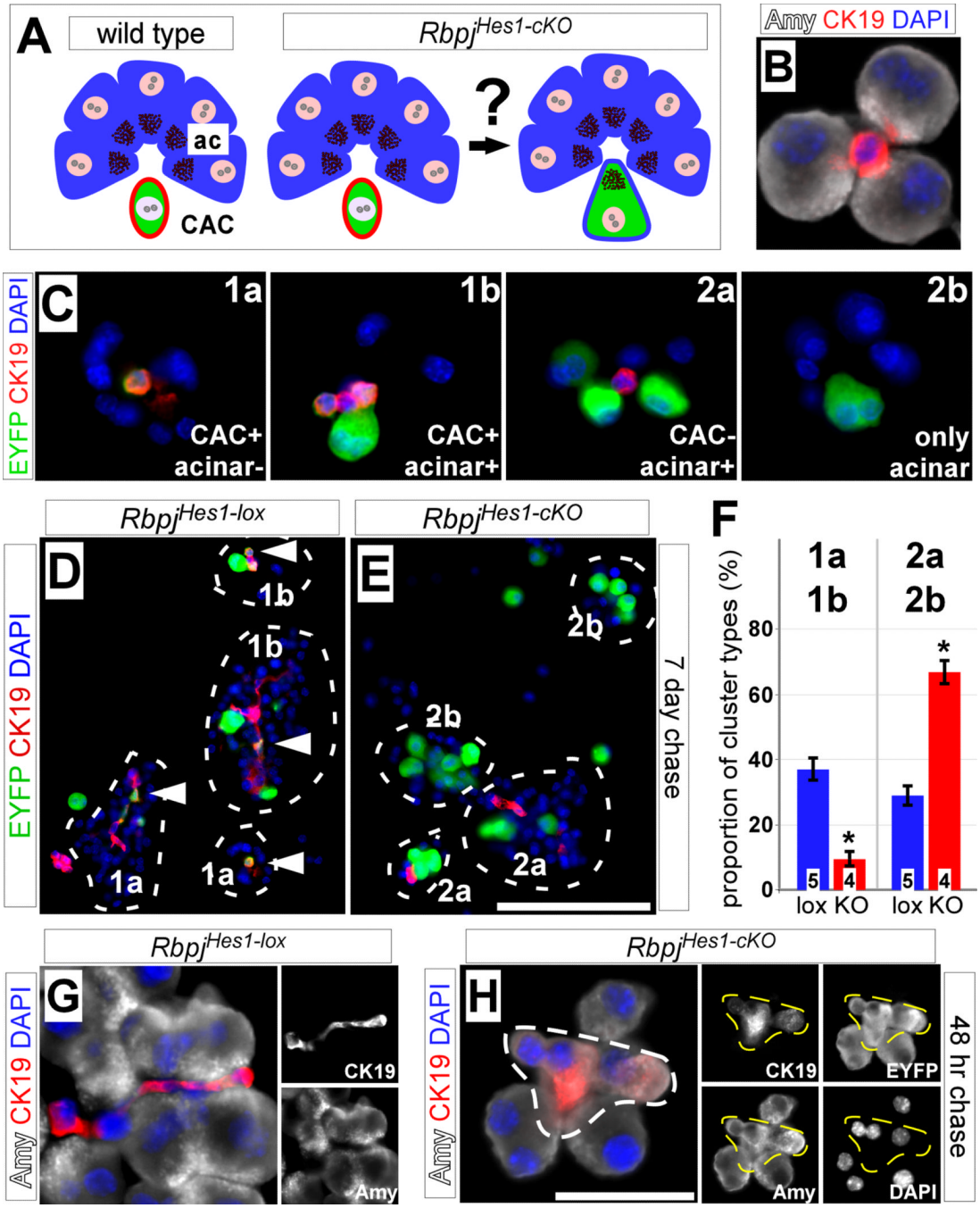

Figure 5. *Hes1*$^{+}$ CACs contribute to acinar cells upon *Rbpj* deletion

(A) We hypothesize that the increase in acinar labeling after loss of *Rbpj* is due to CACs adopting an acinar fate. Blue, acinar cells; red, CAC; green, Hes1 lineage-labeling. **(B)** Dissociation of whole pancreata generates small clusters containing amylase^{+} acinar cells (white) and CK19^{+} CACs (red). **(C)** Clusters from *Hes1* lineage traced (green) pancreata were divided into two major categories, based on the presence (class 1) or absence (class 2) of labeled CACs as indicated. Class 1 clusters contain EYFP^{+} CACs with acinar cells unlabeled (1a) or EYFP^{+} CACs and acinar cells together (1b), while class 2 clusters contain EYFP^{+} acinar cells with unlabeled CACs (2a) or EYFP^{+} acinar cells with no CACs present (2b). Inserts represent schematic representations of cluster types. **(D–E)**

Immunofluorescence for EYFP (green) and CK19 (red) of clusters from dissociated pancreata of *Rbpj*$^{Hes1\text{-}lox}$ and *Rbpj*$^{Hes1\text{-}cKO}$ animals at 7 days post-TM. Only clusters containing 3 or more closely-attached acinar cells were scored (circle). Most of the *Rbpj*$^{Hes1\text{-}lox}$ clusters contain labeled CAC (arrowhead) and belong to class 1, while CACs are either unlabeled or absent altogether in *Rbpj*$^{Hes1\text{-}cKO}$ clusters (classes 2a and 2b). **(F)** Scoring of cluster types from two independent experiments demonstrates a shift in the proportion of clusters from type 1a and 1b to 2a and 2b between *Rbpj*$^{Hes1\text{-}lox}$ and *Rbpj*$^{Hes1\text{-}cKO}$ mice (* $P<0.0005$). Note that the denominator represents the number of total clusters present per field, including entirely EYFP-negative ones. **(G–H)** Immunofluorescence for amylase (white) and CK19 (red) of cell clusters from *Rbpj*$^{Hes1\text{-}lox}$ (J) and *Rbpj*$^{Hes1\text{-}cKO}$ (K) pancreata 48 hrs after TM administration. In *Rbpj*$^{Hes1\text{-}lox}$ mice (J), CK19 and amylase expression are restricted to CAC and acinar cells, respectively. After TM induction (K), some amylase^{+} acinar cells are also positive for CK19 (dotted outline). Co-expression of duct and acinar markers is seen only in EYFP^{+} cells (right). Right, single-channel amylase, CK19, EYFP and DAPI staining as indicated. Numbers in bars (I) indicate mice analyzed per group. Scale bar: D–E, 50 μm; G–H, 25 μm.